



Sustainable production of graphene oxide with ascorbic acid reduction: characterization and insights

Thaddeus Lee^{a,b}, Chun Hui Tan^{a,b}, Chai Yan N^{b,c}, Hing Wah Lee^d, Chun Hong Voon^e, Foo Wah Low^{a,b*}

^a Department of Electrical and Electronic Engineering, Lee Kong Chian Faculty of Engineering and Science, Universiti Tunku Abdul Rahman, 43000 Kajang, Selangor, Malaysia

^b Centre for Advanced and Sustainable Materials Research (CASMR), Lee Kong Chian Faculty of Engineering and Science, Universiti Tunku Abdul Rahman, 43000 Kajang, Selangor, Malaysia

^c Department of Mechanical and Material Engineering, Lee Kong Chian Faculty of Engineering and Science, Universiti Tunku Abdul Rahman, 43000 Kajang, Selangor, Malaysia

^d Center for Semiconductor and Thin Film Research, MIMOS Berhad, Technology Park Malaysia, 57000 Kuala Lumpur, Malaysia

^e Institute of Nano Electronic Engineering, Universiti Malaysia Perlis, Kangar, Malaysia

*Corresponding author: lowfw@utar.edu.my

Received 1 April 2024, Revised 21 April 2024, Accepted 19 June 2024

ABSTRACT

In this study, graphene oxide (GO) was synthesized from graphite powder using KMnO_4 and a concentrated mixture of $\text{H}_2\text{SO}_4/\text{H}_3\text{PO}_4$. The obtained GO was subsequently reduced using ascorbic acid. The ratios of H_2SO_4 to H_3PO_4 and KMnO_4 to graphite powder were kept constant. The synthesized GO and reduced graphene oxide (rGO) were evaluated using UV-visible spectroscopy, FT-IR spectroscopy, XRD, SEM, and EDX. The findings showed that processing graphite powder with KMnO_4 at 60 °C for 12 hours resulted in a high degree of oxidation and minimal defects. Furthermore, ascorbic acid, an alternative to highly toxic hydrazine, aided in eliminating oxygen-containing functional groups in the rGO. This study focuses on the properties of GO produced using the improved Hummer's method, and the changes observed after chemical reduction.

Keywords: Graphene Oxide, Reduced Graphene Oxide, Electrical Conductivity

1. INTRODUCTION

GO and rGO, derived from graphene, have been extensively studied because of their notable optical, electrical, mechanical, and thermal properties. Graphene, a single two-dimensional sheet of graphite, is seen as the precursor to other carbon materials like carbon nanotubes and fullerenes. GO and rGO have garnered significant attention in the field of two-dimensional materials because of their distinctive properties [1].

Furthermore, graphene derivatives (GO, rGO) and their combinations with metals and metal oxides have sparked research interest. These materials have demonstrated effectiveness in various fields, including sensors, solar cells, and water purification [2]. Moreover, graphene and GO demonstrate significant potential in improving the mechanical properties of high-temperature materials. Some research has concentrated on examining the impact of GO on metal alloys and ceramics, especially in high-temperature conditions [3].

GO, a non-conductive hydrophilic carbon material is typically obtained through the exfoliation of graphite using strong oxidizing agents. The Hummers' method, which involves the use of KMnO_4 , NaNO_3 , and H_2SO_4 , is the most commonly used procedure for preparing GO [4]. However,

it is often necessary to restore the conductivity of GO and transform it into a conductive graphitic material. This can be accomplished through chemical reduction, such as converting to chemically altered graphene [5]. Researchers are actively working on improving these processes by minimizing the use of toxic materials, reducing the release of toxic gases, minimizing the risk of explosion, and minimizing defects in the resulting graphitic structure [6].

One improvement involves using ascorbic acid instead of hydrazine to reduce GO to rGO. Hydrazine and ascorbic acid operate through different mechanisms and have distinct properties in the reduction of graphene oxide. Hydrazine, a common antioxidant, typically forms hydrazone with carbonyl groups and is widely used in industry despite its high toxicity. When used to reduce graphene oxide, it results in highly hydrophobic graphene with a low oxygen content. The reduction mechanism involves a direct nucleophilic attack of hydrazine on an epoxide group, leading to a series of transformations and the formation of a double bond [7]. In contrast, ascorbic acid is a safe and common essential nutrient exhibiting antioxidant properties. The reduction mechanism of ascorbic acid involves a two-step $\text{S}_{\text{N}}2$ nucleophilic reaction followed by a thermal elimination, resulting in the conversion of graphene oxide to reduced

graphene oxide. Ascorbic acid also has the advantage of achieving a similar level of reduction as hydrazine without the associated toxicity [8]. Additionally, as ascorbic acid only contains carbon, oxygen, and hydrogen, it minimizes the risk of introducing foreign atoms into the reduced products that were not initially present [9].

In addition to the usage of ascorbic acid instead of hydrazine, an improved Hummers' method will be employed. Unlike the original Hummers' method, which uses KMnO_4 , NaNO_3 , and H_2SO_4 , this method omits NaNO_3 and increases the KMnO_4 quantity. It has been shown to produce chemically converted graphene with similar electrical conductivity to the original method, without generating toxic gases and while maintaining an easily controlled temperature. This improved synthesis method may be advantageous for large-scale GO production and subsequent manufacturing of graphene derivative-based devices [6].

The objective of this study is to create well-oxidized GO from graphite powder, utilizing the improved Hummers' method, followed by reduction using safe and environmentally friendly chemicals i.e., ascorbic acid. The GO and rGO are characterized using various spectroscopic and analytical techniques to determine the efficacy of the oxidation, exfoliation, and reduction process.

2. METHODOLOGY

2.1. Materials

Materials: Graphite powder (<math> <20 \mu\text{m}</math>), and L-ascorbic acid (>98%) were purchased from Sigma-Aldrich (St. Louis, USA). KMnO_4 (99%) was purchased from Chemiz (Shah Alam, Malaysia). Barium chloride dihydrate (>99%) was purchased from Biobasic (Markham, Canada).

2.2. Preparation of Graphene Oxide

GO was synthesized using the improved Hummers' method. Graphite powder (1.8 g, 1 wt. equivalent) and KMnO_4 (9.6 g, 5 wt. equivalent) were added to a cold mixture of concentrated $\text{H}_2\text{SO}_4/\text{H}_3\text{PO}_4$ (180:20 mL) in a 9:1 ratio. For the exfoliation of graphite in this study, the specific ratios of reactants i.e., $\text{H}_2\text{SO}_4:\text{H}_3\text{PO}_4 = 9:1$ v/v, and graphite powder: $\text{KMnO}_4 = 1:5$ w/w are taken as they have been demonstrated to induce a high degree of oxidation with low defects [10]. The mixture was heated to 50°C with stirring for 12 hours. Afterward, it was cooled to room temperature and 500 mL of cold de-ionized (DI) water was added to halt the reaction. 5 mL of 30% H_2O_2 was added to the mixture. After letting the solid material settle, the supernatant was decanted. The remaining solid was then washed with 5% HCl until SO_4^{2-} ions were removed completely (1 M barium chloride solution no longer produces a white precipitate in the supernatant). The solid material was subsequently rinsed with DI water (3 \times) and ethanol (2 \times). The material was then dispersed in 1.5 L of DI water, and this dispersion was stirred for 12 hours at 60°C . Finally, the material was dried at 60°C for 24 hours, resulting in a brown-black sample.

2.3. Preparation of Reduced Graphene Oxide

Firstly, 0.2 g of GO solid was ground into a powder using a mortar and pestle. This powder was then dispersed in 200 mL of DI water and stirred for 12 hours at 60°C . Following this, 2 g of ascorbic acid was added to the dispersion and stirred for an additional 30 minutes at the same temperature. The resulting black product was collected by centrifugation and then washed with DI water (3 \times) and ethanol (2 \times). Finally, the material was dried at 60°C for 24 hours, yielding a black sample.

3. RESULTS AND DISCUSSION

During the oxidation of graphite, oxygen binds to the graphene layers. This increases their solubility and polarity in water, causing the solution to change color from yellow to brown. The intensity of the brown color is dependent on the concentration of GO. It has been shown that well-oxidized GO exhibits an absorption maximum of 225 nm [11]. In **Figure 1**, the produced GO (blue curve) exhibits a maximum absorption peak at approximately 226 nm due to the π - π transition of the atomic C=C bonds [12]. The reduction of GO was observed using UV-visible spectroscopy. In **Figure 1**, the peak of rGO (red curve) was observed at 238 nm after reduction with ascorbic acid. The shift in absorption from 226 to 238 nm suggests the restoration of electronic conjugation within the graphene sheets following reduction. [13].

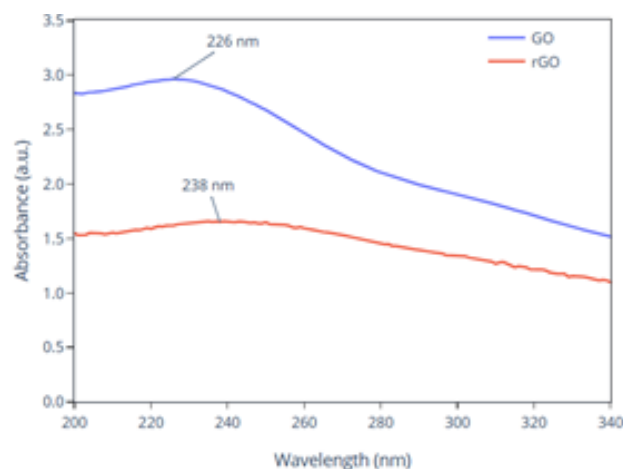


Figure 1. UV-visible spectra of GO and rGO

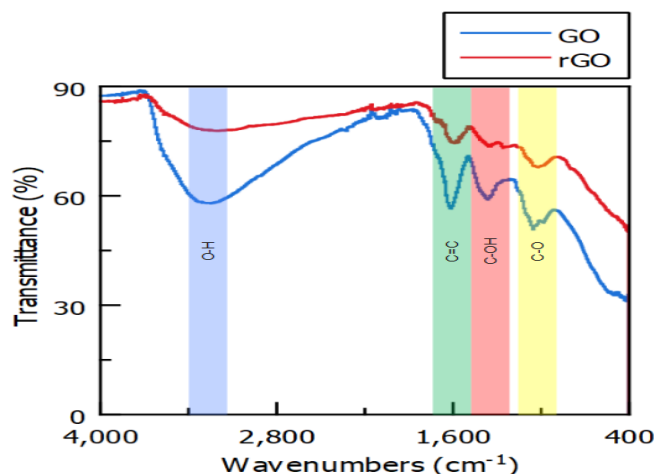


Figure 2. FTIR spectra of GO and rGO

FTIR spectroscopy was utilized to examine the functional groups in GO and rGO. The FTIR spectrum of GO, illustrated in **Figure 2**, exhibits broad peaks within the 1700-1200 cm^{-1} range. This indicates the presence of oxygen functional groups like carboxyl, hydroxyl, and epoxy groups [14]. The intensity of these peaks decreases when GO is reduced to rGO, due to the removal of oxygen functional groups. In the FTIR spectrum of rGO, a weak peak is typically observed around 1600-1500 cm^{-1} , corresponding to sp^2 -hybridized carbon atoms [15, 16].

FTIR spectroscopy was employed to assess the introduction of oxygen-containing functional groups into the carbon lattice. The GO spectrum displayed modes typical of oxygen-containing functional groups. A wide peak at 3253.75 cm^{-1} pointed to the presence of carboxylic acid $\nu(\text{O-H})$ caused by intercalated water [17, 18]. The $\nu(\text{C=C})$ peak at approximately 1,621.42 cm^{-1} indicated the presence of unoxidized graphitic domains [19]. The peak at 1361.44 cm^{-1} is attributed to $\nu(\text{C-OH})$ stretching vibrations [20]. Additionally, $\nu(\text{C-O})$ vibration modes were observed at 1,054 cm^{-1} [12].

When converting GO to rGO, the number of functional groups decreases significantly. Specifically, the reduction process noticeably reduces the peaks associated with oxygen-containing functional groups, although not completely, suggesting the possibility of achieving a higher level of reduction. However, the peak corresponding to the C=C functional group remained relatively intact. This decrease in peak intensity aligns with observations made using UV-visible spectroscopy.

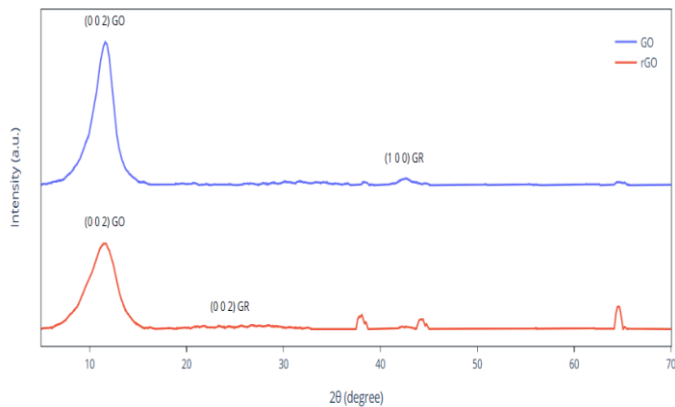


Figure 3. X-ray diffraction patterns of GO and rGO

X-ray diffraction (XRD) patterns were documented for both GO powder and rGO powder. Following the oxidation of graphite, a diffraction peak for GO was detected at $2\theta = 11.4546^\circ$, which corresponds to a layer-to-layer distance of 0.772 nm. This result aligns with existing literature [6, 21], indicating the appearance of oxygen-containing functional groups such as epoxy, carboxyl ($-\text{COOH}$), hydroxyl groups, and inserted H_2O molecules. The peak is associated with the (0 0 2) crystallographic plane of GO. Further, a low-intensity peak at 42.5° is indexed to the (1 0 0) plane of graphite [22].

The reduction of GO is demonstrated by XRD analysis. In **Figure 3**, the diffraction peak of rGO ($2\theta = 11.5400^\circ$) has shifted from that of GO, indicating a layer-to-layer distance of 0.766 nm. This change suggests that the interlayer

distance of rGO slightly decreased after reduction due to the rGO sheets having fewer oxygen-containing functional groups. Moreover, a broad, weakly resolved peak around 25° , corresponding to the (0 0 2) plane of graphite, is also observed. This peak is reported to be the strongest peak in well-reduced and exfoliated graphene sheets [23].

The minor change in the diffraction peak from the (0 0 2) crystallographic plane of GO to rGO, and the weak peak formation around 25° indicates that while there is a chemical reduction of GO, the restoration of conjugation of graphene sheets is not significant [22]. Similar to the slight shift in the UV-visible absorption peak and the modest reduction of FTIR peak intensities, this could be attributed to inadequate reduction and/or the agglomeration and restacking of rGO sheets. The XRD pattern of rGO also exhibited some irregularities, with small peaks observed at 37.9° , 44.2° , and 64.6° . These peaks may be attributed to the presence of trace amounts of aluminium in the rGO powder. In particular, the observed peaks can be directly associated with the (1 1 1), (2 0 0), and (2 2 0) crystallographic planes of aluminium [24].

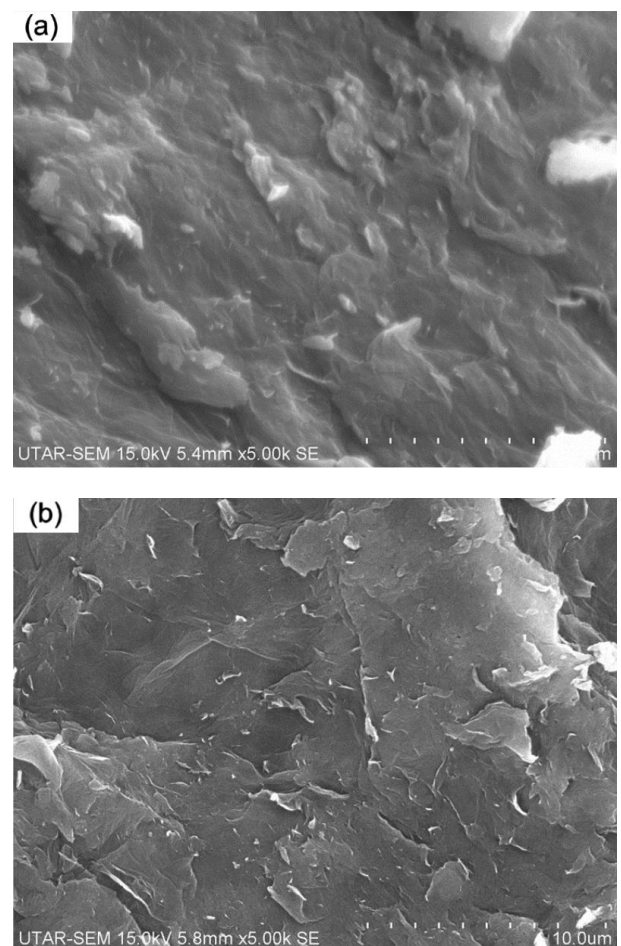


Figure 4. SEM images of (a) GO and (b) rGO flakes imaged at 5k magnification

The morphology of GO before and after reduction was characterized by Scanning Electron Microscopy (SEM), as shown in **Figure 4(a)-(b)**. GO exhibits a crinkly surface with stacked structures, where darker areas indicate the presence of oxygen functional groups [25]. In contrast to the irregular curved edges and folded surface of GO, the rGO

sample shows a lesser degree of stacking, likely due to the delamination of structures during the reduction process. Furthermore, the rGO samples display smaller particle sizes, which are attributed to the reduced interlayer spaces caused by oxygen-containing functional groups [26]. The elimination of these groups leads to rGO particles with increased roughness and sharper edges [27].

Table 1. Elemental composition of GO and rGO

Sample	Mass Percentage of Oxygen	Mass Percentage of Carbon	Atomic Percentage of Oxygen	Atomic Percentage of Carbon
GO	47.30%	52.70%	40.26%	59.74%
rGO	37.84%	62.16%	31.37%	68.63%

Table 1 presents a comparison of the mass percentage and atomic percentage of oxygen and carbon atoms in both GO and rGO powders. This data was obtained from Energy Dispersive X-Ray (EDX) analysis. As GO is reduced to rGO, the percentage of oxygen decreases, and the percentage of carbon increases. The EDX results in Table 1 display the elemental composition of GO and rGO powders, with carbon and oxygen being the main elements detected. The mass percentage of oxygen in GO and rGO powders, relative to the total mass of carbon and oxygen atoms, was estimated to be 47.30% and 37.84%, respectively. Similarly, the atom percentage of oxygen in GO and rGO powders was estimated to be 40.26% and 31.37%, respectively. These results support the observations made using the previously discussed characterization techniques. EDS spectroscopy directly measures the change in oxygen content, indicating that ascorbic acid partially reduced GO to rGO.

Table 2. Electrical conductivity of GO and rGO dispersions

Sample	Conductivity ($\mu\text{S}/\text{cm}$)
GO	~182.0
rGO	~69.4

Dispersions of GO and rGO were prepared at 1 mg/mL by sonicating the respective powders in DI water and then tested using a conductivity meter. Initially, the DI water used to prepare the dispersions was found to have a conductivity of approximately 1.9 $\mu\text{S}/\text{cm}$, serving as a reference point. Subsequently, the conductivities for the GO and rGO dispersions were recorded in **Table 2**. Both dispersions show higher conductivities than pure water, thus demonstrating their electrical conductivity properties.

From previous characterizations, it is evident that the degree of reduction from GO to rGO is modest. This leaves some residual oxygen functional groups that hinder charge carrier mobility and decrease the overall conductivity of rGO [28]. Additionally, rGO sheets may agglomerate or restack more than GO sheets due to van der Waals interactions [29, 30], reducing the effective surface area for

charge transport. This could be exacerbated by inadequate exfoliation of GO before the reduction process. Consequently, the dispersion quality of rGO might be inferior to that of GO, leading to a non-uniform distribution of rGO powder in the solvent and creating localized areas of low conductivity [31, 32]. This issue can counteract the improvements in electrical conductivity achieved by removing oxygen-containing functional groups. These findings clarify that the electrically conductive properties of GO and rGO depend not only on the degree of reduction but also on a complex interplay of factors that ultimately determine the restoration of π -conjugation within the graphitic structure.

4. CONCLUSION

In conclusion, this study successfully produced GO from graphite powder by employing the improved Hummers' method. The GO was then reduced to obtain rGO using ascorbic acid. The characterization of both GO and rGO was performed using various analytical techniques, including UV-visible spectroscopy, FTIR spectroscopy, XRD, SEM, EDS, and conductivity probing. The results show that using KMnO_4 to oxidize graphite powder at 60°C for 12 hours produces GO of good quality and minimal defects. The following reduction process using ascorbic acid aids in eliminating oxygen-containing functional groups in the rGO, thereby reinstating electronic conjugation within the rGO layers.

UV-visible spectroscopy verified the successful reduction of GO to rGO, as indicated by the shift in absorption peaks from 226 nm to 238 nm. Meanwhile, FTIR spectroscopy showed the presence of oxygen-containing functional groups in GO, which decreased in intensity upon reduction to rGO. XRD analysis demonstrated a slight decrease in interlayer distance and the restoration of graphene-like characteristics in rGO compared to GO. SEM images showed the morphological changes from stacked structures in GO to delaminated structures in rGO, with increased roughness and sharper edges. EDS analysis further corroborated the reduction process. It showed a decrease in the percentage of oxygen and an increase in the percentage of carbon in rGO compared to GO. Conductivity measurements were conducted to determine the electrically conductive and dispersion properties of GO and rGO. This helped to elucidate the effects of the chemical reduction of GO.

In summary, this study offers insights into the synthesis and characterization of GO and rGO. The improved Hummers' method, along with the use of ascorbic acid as a reducing agent, presents the potential for producing well-oxidized GO with minimized defects and a safe, environmentally friendly reduction process. Further research can focus on optimizing the reduction process to achieve higher levels of restoration of graphene-like properties in rGO.

ACKNOWLEDGMENTS

The research was supported by the Ministry of Higher Education (MoHE), through the Fundamental Research Grant Scheme (FRGS/1/2022/TK08/UTAR/02/39).

REFERENCES

- [1] C. Kavitha, "A review on reduced Graphene oxide hybrid nano composites and their prominent applications," *Materials Today: Proceedings*, vol. 49, pp. 811–816, 2022.
- [2] X. Huang, X. Qi, F. Boey, and H. Zhang, "Graphene-based composites," *Chem. Soc. Rev.*, vol. 41, no. 2, pp. 666–686, 2012.
- [3] A. Jiříčková, O. Jankovský, Z. Sofer, and D. Sedmidubský, "Synthesis and Applications of Graphene Oxide," *Materials*, vol. 15, no. 3, p. 920, 2022.
- [4] Md. S. A. Bhuyan, Md. N. Uddin, Md. M. Islam, F. A. Bipasha, and S. S. Hossain, "Synthesis of graphene," *Int Nano Lett*, vol. 6, no. 2, pp. 65–83, 2016.
- [5] D. Li, M. B. Müller, S. Gilje, R. B. Kaner, and G. G. Wallace, "Processable aqueous dispersions of graphene nanosheets," *Nature Nanotech*, vol. 3, no. 2, pp. 101–105, 2008.
- [6] D. C. Marcano et al., "Improved Synthesis of Graphene Oxide," *ACS Nano*, vol. 4, no. 8, pp. 4806–4814, 2010.
- [7] C. K. Chua and M. Pumera, "Chemical reduction of graphene oxide: a synthetic chemistry viewpoint," *Chem. Soc. Rev.*, vol. 43, no. 1, pp. 291–312, 2014.
- [8] J. Gao, F. Liu, Y. Liu, N. Ma, Z. Wang, and X. Zhang, "Environment-Friendly Method To Produce Graphene That Employs Vitamin C and Amino Acid," *Chem. Mater.*, vol. 22, no. 7, pp. 2213–2218, 2010.
- [9] M. J. Fernández-Merino et al., "Vitamin C Is an Ideal Substitute for Hydrazine in the Reduction of Graphene Oxide Suspensions," *J. Phys. Chem. C*, vol. 114, no. 14, pp. 6426–6432, 2010.
- [10] A. L. Higginbotham, D. V. Kosynkin, A. Sinitskii, Z. Sun, and J. M. Tour, "Lower-Defect Graphene Oxide Nanoribbons from Multiwalled Carbon Nanotubes," *ACS Nano*, vol. 4, no. 4, pp. 2059–2069, 2010.
- [11] A. A. Balandin et al., "Superior Thermal Conductivity of Single-Layer Graphene," *Nano Lett.*, vol. 8, no. 3, pp. 902–907, 2008.
- [12] Y. Xu, H. Bai, G. Lu, C. Li, and G. Shi, "Flexible Graphene Films via the Filtration of Water-Soluble Noncovalent Functionalized Graphene Sheets," *J. Am. Chem. Soc.*, vol. 130, no. 18, pp. 5856–5857, 2008.
- [13] D. Li, M. B. Müller, S. Gilje, R. B. Kaner, and G. G. Wallace, "Processable aqueous dispersions of graphene nanosheets," *Nature Nanotech*, vol. 3, no. 2, pp. 101–105, 2008.
- [14] IR Spectrum Table & Chart (no date) IR Spectrum Table. Available at: <https://www.sigmaaldrich.com/MY/en/technical-documents/technical-article/analytical-chemistry/photometry-and-reflectometry/ir-spectrum-table> (Accessed: 02 November 2023).
- [15] X. Chen, X. Lai, J. Hu, and L. Wan, "An easy and novel approach to prepare Fe₃O₄-reduced graphene oxide composite and its application for high-performance lithium-ion batteries," *RSC Adv.*, vol. 5, no. 77, pp. 62913–62920, 2015.
- [16] C. Nethravathi and M. Rajamathi, "Chemically modified graphene sheets produced by the solvothermal reduction of colloidal dispersions of graphite oxide," *Carbon*, vol. 46, no. 14, pp. 1994–1998, 2008.
- [17] Z. Mo et al., "Preparation and characterization of a PMMA/Ce(OH)₃, Pr₂O₃/graphite nanosheet composite," *Polymer*, vol. 46, no. 26, pp. 12670–12676, 2005.
- [18] T. F. Emiru and D. W. Ayele, "Controlled synthesis, characterization and reduction of graphene oxide: A convenient method for large scale production," *Egyptian Journal of Basic and Applied Sciences*, vol. 4, no. 1, pp. 74–79, 2017.
- [19] H.-L. Guo, X.-F. Wang, Q.-Y. Qian, F.-B. Wang, and X.-H. Xia, "A Green Approach to the Synthesis of Graphene Nanosheets," *ACS Nano*, vol. 3, no. 9, pp. 2653–2659, 2009.
- [20] A. T. Habte and D. W. Ayele, "Synthesis and Characterization of Reduced Graphene Oxide (rGO) Started from Graphene Oxide (GO) Using the Tour Method with Different Parameters," *Advances in Materials Science and Engineering*, vol. 2019, pp. 1–9, 2019.
- [21] Z. Fan, K. Wang, T. Wei, J. Yan, L. Song, and B. Shao, "An environmentally friendly and efficient route for the reduction of graphene oxide by aluminum powder," *Carbon*, vol. 48, no. 5, pp. 1686–1689, 2010.
- [22] G. M. Neelgund and A. Oki, "Graphene-Coupled ZnO: A Robust NIR-Induced Catalyst for Rapid Photo-Oxidation of Cyanide," *ACS Omega*, vol. 2, no. 12, pp. 9095–9102, 2017.
- [23] X. Jiao, Y. Qiu, L. Zhang, and X. Zhang, "Comparison of the characteristic properties of reduced graphene oxides synthesized from natural graphites with different graphitization degrees," *RSC Adv.*, vol. 7, no. 82, pp. 52337–52344, 2017.
- [24] X. Y. Goh et al., "Advanced Fabrication and Multi-Properties of Aluminum-Based Aerogels from Aluminum Waste for Thermal Insulation and Oil Absorption Applications," *Molecules*, vol. 28, no. 6, p. 2727, 2023.
- [25] L. Stobinski et al., "Graphene oxide and reduced graphene oxide studied by the XRD, TEM and electron spectroscopy methods," *Journal of Electron Spectroscopy and Related Phenomena*, vol. 195, pp. 145–154, 2014.
- [26] S. Azizighannad and S. Mitra, "Stepwise Reduction of Graphene Oxide (GO) and Its Effects on Chemical and Colloidal Properties," *Sci Rep*, vol. 8, no. 1, p. 10083, 2018.
- [27] N. G. De Barros et al., "Graphene Oxide: A Comparison of Reduction Methods," *C*, vol. 9, no. 3, p. 73, 2023.
- [28] L. Lavagna, D. Massella, E. Priola, and M. Pavese, "Relationship between oxygen content of graphene and mechanical properties of cement-based composites," *Cement and Concrete Composites*, vol. 115, p. 103851, 2021.
- [29] D. Konios, M. M. Stylianakis, E. Stratakis, and E. Kymakis, "Dispersion behaviour of graphene oxide and reduced graphene oxide," *Journal of Colloid and Interface Science*, vol. 430, pp. 108–112, 2014.
- [30] M. F. El-Kady, V. Strong, S. Dubin, and R. B. Kaner, "Laser Scribing of High-Performance and Flexible Graphene-Based Electrochemical Capacitors," *Science*, vol. 335, no. 6074, pp. 1326–1330, 2012.

- [31] L.-C. Tang et al., "The effect of graphene dispersion on the mechanical properties of graphene/epoxy composites," *Carbon*, vol. 60, pp. 16–27, 2013.
- [32] M. Majidian, C. Grimaldi, L. Forró, and A. Magrez, "Role of the particle size polydispersity in the electrical conductivity of carbon nanotube-epoxy composites," *Sci Rep*, vol. 7, no. 1, p. 12553, 2017.